The Astronomical Journal, 149:105 (6pp), 2015 March doi:10.1088/0004-6256/149/3/105

IRRADIATION PRODUCTS ON DWARF PLANET MAKEMAKE

M. E. Brown, E. L. Schaller, and G. A. Blake
Division of Geological and Planetary Sciences, California Institute of Technology, Pasadena, CA 91125, USA; mbrown@caltech.edu
Received 2014 November 10; accepted 2015 January 8; published 2015 February 19

ABSTRACT

The dark, reddish tinged surfaces of icy bodies in the outer solar system are usually attributed to the long term irradiation of simple hydrocarbons leading to the breaking of C–H bonds, loss of hydrogen, and the production of long carbon chains. While the simple hydrocarbon methane is stable and detected on the most massive bodies in the Kuiper Belt, evidence of active irradiation chemistry is scant except for the presence of ethane on methane-rich Makemake and the possible detections of ethane on more methane-poor Pluto and Quaoar. We have obtained deep high signal-to-noise spectra of Makemake from 1.4 to 2.5 μm in an attempt to trace the radiation chemistry in the outer solar system beyond the initial ethane formation. We present the first astrophysical detection of solid ethylene and evidence for acetylene and high-mass alkanes—all expected products of the continued irradiation of methane, and use these species to map the chemical pathway from methane to long-chain hydrocarbons.

Key words: Kuiper belt objects: individual (Makemake) – planets and satellites: surfaces – radiation mechanisms: general

Supporting material: data behind figures

1. INTRODUCTION

The red coloring frequently seen on solid objects in the outer solar system is usually attributed to irradiation products of hydrocarbons (Sagan & Khare 1979; Wilson et al. 1994; Cooper et al. 2003). Laboratory experiments have shown, for example, that many different hydrocarbon ices, when exposed to many different types of irradiation, respond by forming a reddish colored refractory residue (Khare et al. 1984; Thompson et al. 1987; Brunetto et al. 2006). Such residues are thought to be composed of long-chain hydrocarbons that form from the selective breaking of C–H bonds and the subsequent removal of the hydrogen atom. Indeed, continued irradiation leads to the darkening and flattening of the spectrum as would be expected for amorphous carbon (Moroz et al. 2004).

The most commonly observed solid hydrocarbon in the outer solar system is methane, which appears in the spectra of objects massive enough to maintain a methane atmosphere against escape (Schaller & Brown 2007b). Methane dominates the spectrum of Neptune's satellite Triton (Cruikshank et al. 1993), and the Kuiper Belt objects (KBOs) Eris (Brown et al. 2005), Pluto (Owen et al. 1993), and Makemake (Brown et al. 2007), and appears in small abundances on the less massive KBOs Quaoar (Schaller & Brown 2007a) and possibly 2007 OR10 (Brown et al. 2011). Methane might also be present on the distant body Sedna (Barucci et al. 2005). These objects all have moderately to strongly red visible colors, suggesting that hydrocarbon irradiation products are dominating the visible reflectance spectrum. Evidence for the presence of intermediate products between methane and the presumed long-chain hydrocarbons that produce the red visible colors has been scant, however. Ethane, one of the first irradiation products of methane, has been detected robustly on Makemake (Brown et al. 2007) and more weakly on Quaoar (Schaller & Brown 2007a) and Pluto (DeMeo et al. 2010; Holler et al. 2014).

Laboratory studies of methane irradiation suggest some of the additional products that should also be present. Bennett et al. (2006) irradiated methane with energetic electrons simulating the effects of cosmic ray bombardment and studied the development of CH_x and C_2H_x species. They suggest that the chemical pathway of methane (CH_4) irradiation involves C–H bond rupture to form methyl radicals (CH_3) which can combine to form ethane (C_2H_6). Excited ethane can undergo unimolecular decomposition to form either the ethyl radical (C_2H_5) or ethylene (C_2H_4) (both of which can also be produced from unexcited ethane via radiolysis). The vinyl radical (C_2H_3) and acetylene (C_2H_2) are then both produced via radiolysis of ethylene. In these experiments, the methane was irradiated at 10 K; upon heating to temperatures more relevant to the Kuiper Belt region, the radicals all combined to form stable molecules. Thus we would expect that the possibly observable methane irradiation products in the Kuiper Belt should include ethane, ethylene, and acetylene.

Gerakines et al. (1996) irradiated pure methane samples with UV photons and identified the same species as detected in the electron irradiation experiments, but also identified the continued growth of longer-chain hydrocarbons through the identification of propane (C_3H_8) and of non-specific bands in the 3.4 μm aliphatic C–H stretching region and the 6–8 μm deformation region.

Dwarf planet Makemake, discovered as part of the wide area Palomar Observatory survey (Brown 2008), is a particularly good object on which to study the effects of methane irradiation. Makemake is the second brightest KBO, after Pluto, so high quality spectra are obtainable. As importantly, the surface of Makemake appears to be dominated by methane in much larger concentrations than on the other large outer solar system objects (Brown et al. 2007; Tegler et al. 2008). Schaller & Brown (2007b) explained the large methane abundance as a consequence of the location of Makemake just at the mass and temperature transition between an object which can retain—and thus be dominated by—a nitrogen atmosphere and an object which has lost significant amounts of nitrogen and is now dominated by the less-volatile methane. This dominance of methane on the surface of Makemake allows for the sintering of very large grains on the surface of this object (Eluszkiewicz et al. 2007). The dominance of methane on the

Table 1
Journal of Makemake Observations

Dates (UT)	*H* band Exposure (hr)	*K* band Exposure (hr)	Airmass Range	Calibrator/Type
2005 Apr 24–25	1.33	4.07	1.22–1.02	HD 109464/F84
2006 Dec 28–29	⋯	2.67	1.09–1.01	HD 112257/G6V
2007 Apr 25–27	3.5	6.08	1.36–1.01	HD 102142/G7V
2010 Apr 22	2.00	⋯	1.05–1.01	HD 102142/G7V
2013 May 22–23	7.83	⋯	1.39–1.01	HD 117302/G3V

surface also presumably greatly enhances the efficiency of radiolytic processing. On objects such as Pluto and Triton and perhaps Eris, nitrogen is the dominant species and methane is largely diluted in a solid state solution. The radiolytic chemistry discussed above, which begins with the reaction of two adjacent methyl radicals, would be greatly inhibited in these diluted methane solutions. Makemake, in contrast, should potentially show a much richer detectable irradiation chemistry. Indeed, the early spectroscopy of Makemake which identified ethane suggested that additional absorbers could also be present, but these species were not identifiable at the signal-to-noise then available (Brown et al. 2007).

To explore irradiation chemistry on Makemake and to test the suggestion that additional absorbers are present in the spectrum, we have obtained spectra of Makemake with significantly enhanced signal-to-noise. Here we present the spectrum and our identification of species present and discuss implications for the surface of Makemake and for irradiation in the outer solar system.

2. OBSERVATIONS

We obtained medium resolution ($R \sim 2500$) spectra of the *H* and *K* band regions of Makemake on 10 good nights over a period of 9 yr using NIRSPEC, the facility medium to high resolution spectrometer at the Keck telescope (McLean et al. 1998). With a total integration time of 16.2 hr in *H* band and 13.2 hr in *K* band, these observations increase the total integration by factors of 12 and 3 in *H* and *K* bands, respectively, from those presented in Brown et al. (2007). For all observations, the target was identified by its motion with respect to the fixed stars, centered into the 0.57 arcsec slit, and tracked using the infrared slit guiding camera. All observations consisted of series of 240–300 s integrations on two alternating nod positions along the slit. Observations were obtained between airmass of 1.4 and 1.0, and telluric calibration was performed by dividing by the spectrum of nearby solar type stars observed within 0.1 airmasses of the target observation (Table 1). Data reduction was performed as described in Brown et al. (2007) with the better optimized spectral extraction described by Brown & Rhoden (2014). Though these measurements only record relative reflectance values, we convert them to absolute reflectance by scaling the full visible to near-infrared spectrum from Brown et al. (2007) to the visible albedo of 81% (Ortiz et al. 2012; Brown 2013) and matching the current spectra (Figure 1). As found earlier, the spectrum of Makemake is dominated by broad saturated absorption features of methane consistent with transmission through ~centimeter path lengths.

Care was taken to minimize systematic errors in the spectra and reductions. In particular, the use of multiple spectra over multiple years, each with a different calibrator source, allows us to minimize calibrator-to-calibrator inconsistencies. The restriction of the data set to spectra obtained at low airmass prevents major transmission differences between the spectra. Bad pixels are automatically flagged and removed in the data reduction, but we examined each spectral image by hand to identify any that missed the automatic cut. The resulting spectra have been examined by hand to ensure that there are no spurious features above the level of the noise that could possibly be attributed to telluric features. Some systematic features inevitably remain, including occasional unremoved bad pixels and small errors in the continuum slopes, but neither of these features will affect our spectral identification.

3. SPECTRAL MODELING

3.1. K Band

The strongest deviation from the methane spectrum is in the region beyond 2.25 μm, where most of the potential irradiation products have their strongest overtone bands (stronger fundamental bands could be found beyond 3 μm, but Makemake is too faint for current telescopes to observe at these longer wavelengths). Figure 1 shows the *K* band spectrum of Makemake compared to a model methane spectrum. This model (and subsequent spectral models) is constructed using the bidirectional scattering theory of Hapke (1993), and the surface is modeled as one that consists of a spatially segregated mixture of highly backscattering 2 cm grains of methane covering 80% of the visible surface and a nonphysical featureless continuum with 100% reflectance covering the remaining 20% of the surface. Additional absorption features are clearly present in the spectrum, particularly in the region beyond 2.2 μm.

The difference between the true spectrum and the model spectrum helps show what additional absorption features are needed to explain the true spectrum (Figure 2). To better pick out the broad expected absorption features, we also show the spectrum convolved with a Gaussian function with a FWHM of 6 pixels, giving an effective resolution of approximately $R = 1000$. Superimposed on the Makemake difference spectrum, we also show synthetic spectra of the proposed irradiation products ethane and ethylene. We construct these synthetic spectra using the optical constants of Hudson et al. (2014) for acetylene and from pre-publication measurements by Hudson et al. available on the internet.[1] For these synthetic spectra we assume 10 μm grain sizes and isotropically scattering grains. We also show measured reflectance spectra of propane and paraffin from Clark et al. (2009). Paraffin is mixture of long chain hydrocarbon alkanes with lengths

[1] http://science.gsfc.nasa.gov/691/cosmicice/constants.html

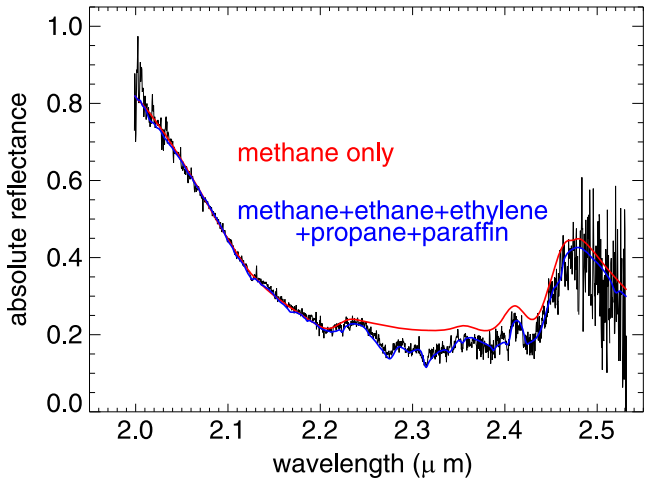

Figure 1. *K* band spectrum of Makemake fits a model of a spectrum of methane ice with 2 cm-sized grains (red). The deviation beyond 2.2 μm is well fit by absorption due to the expected irradiation products of methane: ethane, ethylene, and higher-mass alkanes (blue). The data used to create this figure are available.

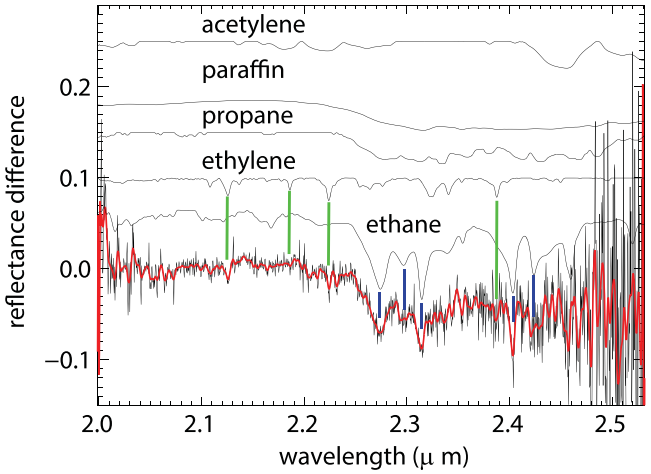

Figure 2. Deviation of the spectrum of Makemake from that of a methane model shows other absorption which might also be present. Spectrum of predicted irradiation products account for most of the additional spectral absorption. Clear detections of lines of ethane are marked in blue, while lines of clear detections of lines of ethylene are marked in green. Additional indications of ethylene absorption appear at every location of a moderately strong predicted ethylene line, although some blends with ethane and other species make definitive identification of these lines more difficult. The red line shows the Makemake spectrum convolved with a Gaussian function to have an effective resolution of $R \sim 1000$.

typically between 20 and 40 carbon atoms. While these two spectra appear distinctly different from that of ethane, alkanes with increasing carbon numbers from propane appear broadly similar in this wavelength range with a slow shift to a paraffin-like appearance for heavier alkanes. We thus use the combined spectra of propane and paraffin as a proxy for mixtures of long chain alkanes.

As previously suggested, the spectrum of solid ethane provides an excellent fit to the non-methane portion of the spectrum of Makemake. While the previous identification was based primarily on the presence of the 2.273 and 2.314 μm absorption features, at higher signal-to-noise and with spectral coverage to longer wavelengths we clearly see these absorption lines as well as those at 2.296, 2.339, 2.403, 2.424, and 2.459 μm. The identification of ethane on Makemake is incontrovertible.

Another product clearly visible is ethylene. The 2.109 and 2.225 μm absorption features, detected at 2.9σ and 5.1σ above the noise level, respectively, are two of the strongest identifiable absorption features in the otherwise generally smooth region of the spectrum between 2.10 and 2.20 μm. A careful examination also shows the presence of the strong ethylene lines at 2.224 μm (5.3σ) and 2.389 (7.3σ), a tentative detection of the weak line at 2.186 μm (1.2σ), and signs of the blended lines at 2.266, 2.326, and 2.341 μm which are near stronger ethane lines and thus difficult to quantitatively measure. In the highest signal-to-noise region between 2.08 and 2.27 μm, five ethylene features are seen at precisely the predicted wavelengths and at the correct approximate ratios; no predicted ethylene lines are unobserved. In this same region three additional unidentified features of similar depth also appear (2.206, 2.214, 2.232 μm). The probability of a spectral misidentification of ethylene appears miniscule. These observations are the first reported astrophysical detections of solid ethylene. The close match to the wavelengths of the laboratory data shows that ethylene—like ethane—is present in pure form rather than dissolved in a nitrogen matrix. A careful examination of the three unidentified features suggests that they appear on multiple occasions and are real features, but they could not be matched with known spectral features.

Figure 3(a) shows a fit of a linear combination of ethane and ethylene to the Makemake difference spectrum. In this linear model, the ethane and ethylene abundances are 20% and 3% of the abundance of methane, respectively. Additional absorption is clearly required in the longer wavelength region. Acetylene, which should be produced along with ethylene, has a moderately weak absorption in the lower signal-to-noise 2.44 μm region of the spectrum, so it is expected to be undetectable. The absorptions due to propane and paraffin have significant overlap with those of ethane, but while ethane has a few strong distinct lines, the heavier alkanes tend to just have broad absorption beyond 2.25 μm. In Figure 3(b) we add propane and paraffin to our spectral model. In our linear model, the abundances of ethane, ethylene, propane, and paraffin compared to methane are 20, 3, 0.8, and 4%, respectively. An important caveat to keep in mind is that while the spectral modeling used to create synthetic spectra of methane, ethane, and ethylene allows us to specify the fractional contributions with moderate accuracy, the use of measured reflectance spectra for propane and paraffin makes quantitative comparison of the relative contributions of these molecules more uncertain. Comparison of the model to the difference spectrum and of the full model to the absolute spectrum in Figure 1 shows an excellent fit. The presence of higher mass alkanes is strongly implied by the need for broad absorption beyond 2.25 μm, and propane and paraffin fit the spectrum well, but the lack of distinct absorption features due to these hydrocarbons makes definitive identification difficult.

3.2. H Band

The absorption features of the irradiation products are, in general, less strong in the *H* band than in the *K* band, so *H* band is mostly useful as a check that our identifications in the *K* band are correct. Figure 4 shows the *H* band spectrum of Makemake compared to a pure methane model. The strongest deviation in the 1.69 μm region is once again due to ethane. Figure 5 shows

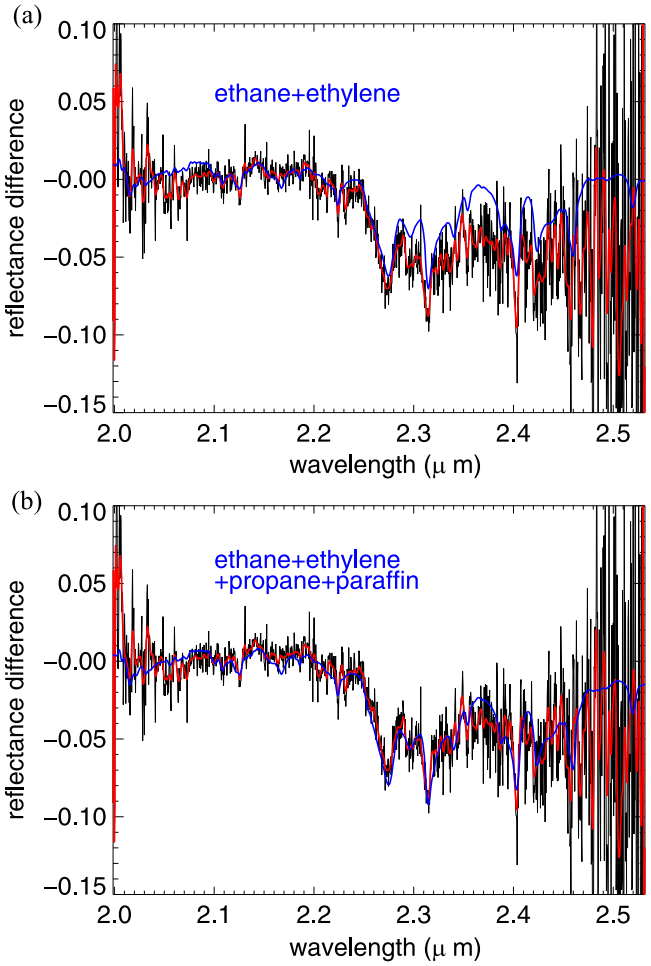

Figure 3. (a) Spectrum of ethane plus ethylene (blue) fits most of the major absorption features of the Gaussian convolved difference spectrum of Makemake (red). (b) The addition of propane and paraffin, as proxies for long-chain alkanes, significantly improves the fit to the difference spectrum.

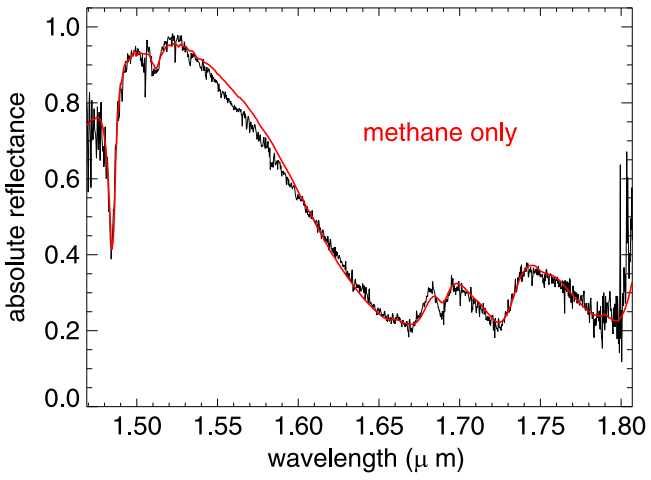

Figure 4. Much of the *H* band spectrum of Makemake is moderately well fit to methane with 3.5 cm grain sizes. The data used to create this figure are available.

the difference spectrum along with the same ethane plus ethylene model used to describe the *K* band data. Ethylene absorption at these wavelengths is sufficiently weak that its effects are not visible. Longer chain alkanes have spectra that

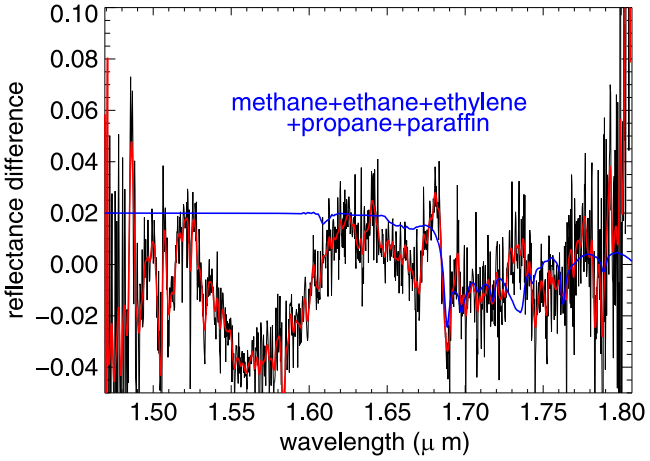

Figure 5. Species identified from the *K* band spectrum have weak absorptions beyond 1.65 μ. The deviation of the Makemake spectrum from a pure methane spectrum (and the lower resolution Gaussian convolved spectrum in red) shows the signature of these species, though the spectral fit in the *H* band is poor compared to the excellent fit in the *K* band. In particular, significant absorption unaccounted for by methane or any other of the modeled features appears shortward of 1.65 μm.

are too similar to that of ethane to be separately identified. The spectral fit in the region beyond 1.65 μm is only moderately good. The strong ethane lines at 1.698, 1.717, and 1.731 μm are clearly present, but the continuum match is not good and an ethane line at 1.734 μm is absent. Lines of ethylene, propane, and paraffin are too weak to observe distinctly in this spectral region.

Unlike in the *K* band, the *H* band absorption due to acetylene occurs in the high signal-to-noise region of the spectrum centered around 1.55 μm. Indeed, a search for this feature was our primary motivation for the emphasis on *H* band spectroscopy in our observations. This region contains one of the largest deviations between the spectrum and the methane model. Hudson et al. (2014) point to this deviation at low signal-to-noise in Brown et al. (2007) as a potential consequence of acetylene and provide new measurements of the optical constants of this ice. With a factor of 12 greater integration time, the deviation from the methane model can now clearly be seen in Figures 4 and 5.

The precise shape of the deviation depends in detail on the methane modeling, which, in turn, depends highly on the additional absorptions beyond 1.67 μm. As can be seen in Figures 4 and 5, the spectral modeling beyond 1.67 μm fits poorly compared to the spectral fit of the *K* band data. We suspect that the poor fit at these wavelengths is dominated by compositional and spectral modeling uncertainties which affect these wavelengths strongly. Methane, on the other hand, is the sole modeled absorber with significant absorption shortward of 1.67 μm. So to model methane independently from the uncertainties of the longer wavelength absorbers, we examine just the 1.47 to 1.63 μm region to find a local best-fit methane only model. The extra absorption required from 1.54 to 1.60 μm is apparent (Figure 6). Acetylene absorbs precisely in this range. A synthetic spectrum of 100 μm grain-sized acetylene using an equal combination of the amorphous and crystalline optical constants from Hudson et al. (2014) is also shown in Figure 6. Adding this spectrum at the 5% abundance level compared to methane provides a much better fit to the data.

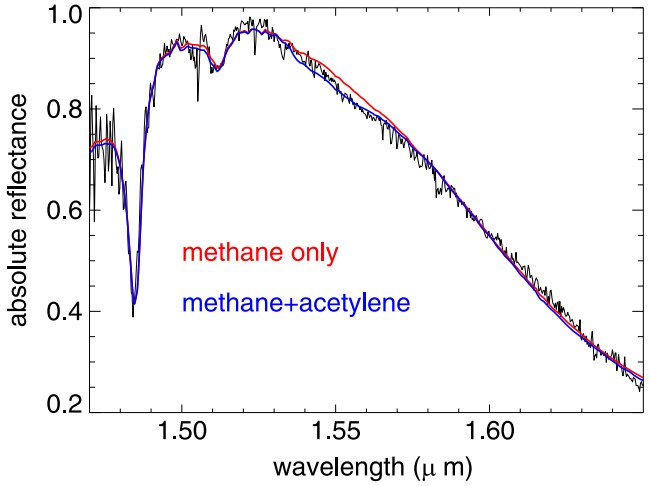

Figure 6. Better fit to the methane-only spectrum occurs if the uncertain and poorly fitting regions beyond 1.65 μm are ignored (blue). In this spectrum the main deviation occurs in the 1.54 μm where acetylene has a strong absorption feature. A model including acetylene provides a better fit to the data (red). No other methane-ice-containing object in the solar system has a broad downward deviation around 1.54 μm.

Identification of acetylene by a broad deviation from a model spectrum is less satisfying than the unambiguous detections in the *K* band of multiple narrow emission features of ethane and ethylene, for example. To explore the possibility that the spectral mismatch is instead a result of poor methane absorption coefficient measurement in this region, we examine the spectra of the other three methane ice rich objects in the outer solar system: Triton, Eris, and Pluto. Examining the spectra of these objects from Cruikshank et al. (1993), Quirico et al. (1999), Rudy et al. (2003), Merlin et al. (2009), we find that in all cases the methane models (modified to include dissolution in N_2 ice for Triton and Pluto) provide excellent fits in the 1.54 to 1.60 μm region (with the exception of the clearly detected CO line at 1.579 μm at Pluto and Triton, which is not present in the Makemake spectrum). The spectrum of Makemake is an exception. While the methane model fits in most places, extra absorption is required precisely in the region in which absorption from acetylene absorbs. While this identification is still less definitive than that of ethane and ethylene, the presence of acetylene on the surface of Makemake appears likely.

4. DISCUSSION

Makemake shows clear evidence of the irradiation processing of methane into longer-chain hydrocarbons. The combination of methyl radicals into ethane molecules is clearly identified, as is the continued irradiation of ethane to make ethylene. Acetylene, an irradiation product of ethylene, is also likely detected.

Creation of long-chain hydrocarbons requires continued creation of high mass hydrocarbons beyond ethane. The spectra of Makemake clearly require absorption in the region beyond 2.25 μm, where propane and higher mass alkanes have overtone bands. The presence of these ices also seems likely.

Precise quantitative abundances of ethane, ethylene, acetylene, and higher mass alkanes are impossible to assess with reflectance spectroscopy. Nonetheless, the spectral models imply a few to tens of percents of these irradiation products. It is interesting to compare the abundances of these irradiation products with the abundances expected from laboratory measurements. Objects in orbits such as Makemake's experience approximately 100 eV (methane molecule)$^{-1}$ over the age of the solar system (Cooper et al. 2003). The experiments of Bennett et al. (2006) only achieved a dosage of 1.6 ev molecule^{-1}, and methane destruction and ethane production were low (and still increasing as irradiation stopped), with a total methane destruction rate of 4% and an abundance of ethane of 0.4% compared to methane. Extrapolating to 100 ev molecule^{-1} doses suggests a fractional ethane abundance of 25%, quite close to our suggested value of approximately 20%. Irradiation by 30 keV protons to 105 eV molecule^{-1} (Baratta et al. 2002) shows nearly complete methane destruction (94%) but with only a 3% abundance of ethane.

While we do not know the fraction of Makemake's original methane currently remaining, Makemake clearly has abundant methane presently, and a higher ethane abundance than would be predicted from the full proton irradiation experiment. One intriguing possible explanation is that Makemake's highly eccentric orbit allows recycling and refreshing of the methane surface once every orbital time scale (309 yr). Methane that is destroyed goes to the formation of dark refractory residues while fresh methane is exposed seasonally. The ethane abundance, in this case, should be closer to a linear extrapolation of the low dosage experiment which, indeed, gives a value very close to that measured. Such an extrapolation of the low dosage irradiation experiment would predict an approximate ethylene abundance of 8%, compared to our model of 3% surface coverage, and an approximate acetylene abundance 1%, compared to our model of 5% surface coverage. We regard these predicted and measured abundances as well within the model uncertainties of both the experimental extrapolation and the spectral modeling and thus consider the matches adequate.

Propane and higher mass alkanes were not measured in the low dosage electron irradiation experiments, so direct comparison is difficult. In the full-dosage proton irradiation experiments, however, the propane abundance exceeded that of ethane by the end of the experiment. Even with the large uncertainties in abundances and in extrapolations, it appears that the propane abundance on Makemake is much lower than expected for irradiation over the age of the solar system. Propane and higher mass alkanes are significantly less volatile than methane, so they will form part of the seasonal lag deposit left behind by methane evaporation and redeposition. A quantitative prediction of how the eccentric orbit, surface temperature changes, and different volatilities of these molecules affects the surface abundance is not currently possible. Modeling of seasonal volatile transport on Makemake is clearly an area with rich possibility.

The observations here show a striking validation of the beginning stages of the expected chemical pathways from methane to dark red refractory residues on objects in the outer solar system. The continued irradiation chemistry to higher mass alkanes beyond ethane is difficult to assess with the weak and overlapping overtone bands available in the *H* and *K* band regions studied here. Significant progress will be made from 3–5 μm spectra of Makemake, where more complex organic molecules have distinctive bands. Such spectra are beyond the capabilities of any current telescopes, but such longer wavelength spectra of Makemake would be a prime target for

future instruments such as NIRSpec on the *James Webb Space Telescope*.

REFERENCES

Baratta, G. A., Leto, G., & Palumbo, M. E. 2002, A&A, 384, 343
Barucci, M. A., Cruikshank, D. P., Dotto, E., et al. 2005, A&A, 439, L1
Bennett, C. J., Jamieson, C. S., Osamura, Y., & Kaiser, R. I. 2006, ApJ, 653, 792
Brown, M. E. 2008, in The Solar System Beyond Neptune, ed. M. A. Barucci et al. (Tucson, AZ: Univ. Arizona Press), 335
Brown, M. E. 2013, ApJL, 767, L7
Brown, M. E., Barkume, K. M., Blake, G. A., et al. 2007, AJ, 133, 284
Brown, M. E., Burgasser, A. J., & Fraser, W. C. 2011, ApJL, 738, L26
Brown, M. E., & Rhoden, A. R. 2014, ApJL, 793, L44
Brown, M. E., Trujillo, C. A., & Rabinowitz, D. L. 2005, ApJL, 635, L97
Brunetto, R., Barucci, M. A., Dotto, E., & Strazzulla, G. 2006, ApJ, 644, 646
Clark, R. N., Curchin, J. M., Hoefen, T. M., & Swayze, G. A. 2009, JGRE, 114, 3001
Cooper, J. F., Christian, E. R., Richardson, J. D., & Wang, C. 2003, EM&P, 92, 261
Cruikshank, D. P., Roush, T. L., Owen, T. C., et al. 1993, Sci, 261, 742
DeMeo, F. E., Dumas, C., de Bergh, C., et al. 2010, Icar, 208, 412
Eluszkiewicz, J., Cady-Pereira, K., Brown, M. E., & Stansberry, J. A. 2007, JGRE, 112, E06003
Gerakines, P. A., Schutte, W. A., & Ehrenfreund, P. 1996, A&A, 312, 289
Hapke, B. 1993, Theory of Reflectance and Emittance Spectroscopy in Topics in Remote Sensing (Cambridge, UK: Cambridge Univ. Press)
Holler, B. J., Young, L. A., Grundy, W. M., Olkin, C. B., & Cook, J. C. 2014, Icar, 243, 104
Hudson, R. L., Ferrante, R. F., & Moore, M. H. 2014, Icar, 228, 276
Khare, B. N., Sagan, C., Arakawa, E. T., et al. 1984, Icar, 60, 127
McLean, I. S., Becklin, E. E., Bendiksen, O., et al. 1998, in SPIE Conf. Ser. 3354 Infrared Astronomical Instrumentation, ed. A. M. Fowler (Bellingham, WA: SPIE), 566
Merlin, F., Alvarez-Candal, A., & Delsanti, A. 2009, AJ, 137, 315
Moroz, L., Baratta, G., Strazzulla, G., et al. 2004, Icar, 170, 214
Ortiz, J. L., Sicardy, B., Braga-Ribas, F., et al. 2012, Natur, 491, 566
Owen, T. C., Roush, T. L., Cruikshank, D. P., et al. 1993, Sci, 261, 745
Quirico, E., Doute, S., Schmitt, B., et al. 1999, Icar, 139, 159
Rudy, R. J., Venturini, C. C., Lynch, D. K., et al. 2003, PASP, 115, 484
Sagan, C., & Khare, B. N. 1979, Natur, 277, 102
Schaller, E. L., & Brown, M. E. 2007, ApJL, 670, L49
Schaller, E. L., & Brown, M. E. 2007, ApJL, 659, L61
Tegler, S. C., Grundy, W. M., Vilas, F., et al. 2008, Icar, 195, 844
Thompson, W. R., Murray, B. G. J. P. T., Khare, B. N., & Sagan, C. 1987, JGR, 92, 14933
Wilson, P. D., Sagan, C., & Thompson, W. R. 1994, Icar, 107, 288